

optical sensitivity of this switch obviates the need for any electrical bias.

Antenna patterns were measured at 200, 375 and 650 MHz for different light intensities on the switch. As Fig. 2 predicts, illumination increased the gain at 200 MHz while decreasing it at 375 MHz. Total gain changes were +12 dB at 200 MHz and -8 dB at 375 MHz with 10 mW illumination. Antenna patterns did not change with optical power at these resonances. At 650 MHz the antenna moves into the second resonance region with increasing optical power. Fig. 4 shows the resulting drastic change in pattern with as little as a microwatt of optical power.

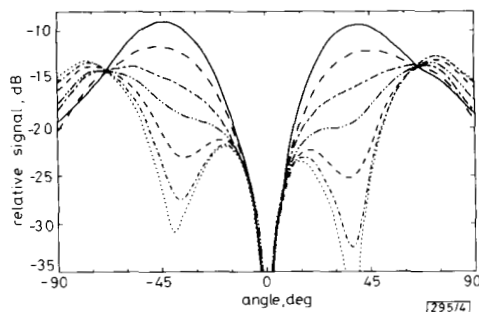


Fig. 4 Pattern of two-segment antenna at 650 MHz as function of optical power on switch

- 10 mW
- - - 52 μ W
- · - · 1.2 μ W
- · - · 0.19 μ W
- · - · 13 nW
- · - · < 8 nW
- · - · dark

Because of power handling limitations of our present switch designs (peak signal less than ~ 1 V), optoelectronically reconfigurable antennas are most suitable for receive applications. However, they can be used for modest transmission of power (several milliwatts).

Clearly the optoelectronic switch exerts significant control over antenna parameters such as gain, pattern, and impedance. Multisegmented monopoles have also been analysed and are being tested.

Summary: We have demonstrated reconfiguration of linear antennas using simple optoelectronic switches. Gain, pattern shape and input impedance can be controlled by the intensity of light impinging on the switches. Many applications involving linear receiving antenna elements, either individually or in ensemble, are possible. Other optically controlled devices are available offering different tradeoffs in response time, sensitivity, size, maximum signal voltage, resistance and capacitance. The key requirement is that the devices do not need bias or other wires that intrude on the electromagnetic fields being controlled.

10th June 1992

J. L. Freeman, B. J. Lamberty and G. S. Andrews (Boeing Defense and Space Group, PO Box 3999, MS 7J-56, Seattle, WA 98124, USA)

References

- 1 DEMPSEY, R. C., and BEVENSEE, R. M.: 'The synaptic antenna for reconfigurable array applications—description'. AP-S Int. Symp. 1989 Dig., Vol. 2, pp. 760–763
- 2 BEVENSEE, R. M., and DEMPSEY, R. C.: 'The synaptic antenna for reconfigurable array applications—behavior'. AP-S Int. Symp. 1989 Dig., Vol. 2, pp. 764–767
- 3 DARYOUSH, A. S., HERCZFELD, P. R., and ROSEN, A.: 'Light controlled antennas'. US Patent No. 4 751 513, 14th June 1988
- 4 DARYOUSH, A. S., BONTZOS, K., and HERCZFELD, P. R.: 'Optically tuned patch antenna for phased array applications'. AP-S Int. Symp. 1986 Dig., Vol. 1, pp. 361–364
- 5 DJORDJEVIĆ, A. R., BAŽDAR, M. B., VITOŠEVIĆ, G. M., SARKAR, T. K., and HARRINGTON, R. F.: 'Analysis of wire antennas and scatterers' (Artech, 1990)

ELECTRONICS LETTERS 30th July 1992 Vol. 28 No. 16

- 6 FREEMAN, J. L., RAY, S., WEST, D. L., THOMPSON, A. G., and LAGASSE, M. J.: 'Microwave control using a high-gain bias-free optoelectronic switch', in YAO, S. K. (Ed.): 'Optical technology for microwave applications', Proc. SPIE, 1991, Vol. 1476, pp. 320–325
- 7 FREEMAN, J. L., RAY, S., WEST, D. L., and THOMPSON, A. G.: 'Optoelectronic devices for unbiased microwave switching'. IEEE MTT-S Int. Microwave Symp. Dig., 1992, pp. 673–676

CONVOLUTIONALLY CODED BINARY PSAM FOR RAYLEIGH FADING CHANNELS

C. Tellambura and V. K. Bhargava

Indexing terms: Amplitude modulation, Fading, Digital communication systems

Recently proposed, pilot symbol assisted modulation (PSAM) uses a known pilot sequence to derive amplitude and phase references at the receiver. The Letter presents convolutional coding for such systems and derives the exact pairwise error probability and the Chernoff upper bound of it. A comparison among PSAM, coherent and differential detected coded systems indicates that, even at 5% Doppler fading rate, coded PSAM requires 3.5 dB more than the ideal coherent case but less than the differential case.

Introduction: In digital mobile communications, fast fading introduces an error floor, degrades BER and inhibits the use of coherent detection. To mitigate these effects, the use of error control coding has been suggested in the literature. However, to realise the full potential benefits of coding, coherent detection is essential. To this end, the use of a tone to provide amplitude and phase reference has been proposed by several authors. Recently, an alternative to the pilot tone technique has emerged, where the transmitter periodically inserts known symbols. The insertion of pilot samples causes a lowering of the data rate and some power loss, which is the price paid for quasicohherent detection. The somewhat ad-hoc proposals of References 2 and 3 have been supplanted by the general analysis in Reference 1. Just as with pilot tone schemes, it has been demonstrated that such a system improves the receiver performance over noncoherent detection and removes error floors [1]. In this Letter, an extension of this scheme to fully interleaved convolutional coding is presented and analysed. Exact pairwise error probability and the Chernoff upper bound for the scheme are derived. Although, for simplicity, we use Rayleigh channel, the analysis can be easily extended to the Rician fading model.

Performance analysis: In the proposed system (Fig. 1), coded binary PSK symbols are interleaved, and the transmitter inserts a known symbol at the beginning of each coded symbol frame of length $M - 1$. As proposed in Reference 1, using K pilot samples, an optimum filter estimates channel gain for each coded symbol bit. The channel gain estimates are then used to form the metric to be used in the Viterbi detector following deinterleaving. As mentioned in Reference 1, the choice of frame size M , number of pilot samples K and optimum filter coefficients is dictated by the anticipated worst

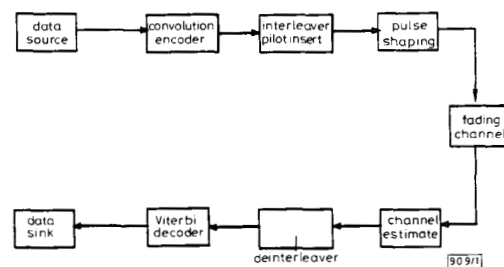


Fig. 1 Coded binary PSAM

1503

case Doppler fading bandwidth and residual frequency offset. In the following, we assume perfect receiver timing, fading to be constant over a bit and, consequently, no intersymbol interference. Also, we assume a negligible residual frequency error.

The transmitted signal can be represented by a complex envelope [1]

$$s(t) = A \sum_{k=-\infty}^{\infty} b(k)p(t - kT) \quad (1)$$

where $p(t)$ is a unit energy pulse, A is an amplitude factor, and T is the symbol duration. We assume, without loss of generality, that pilot symbols are '1'. Hence the received symbol sequence is given by: $b(k) = 1$ for $k = iM$: $\{i = 0, \pm 1, \dots\}$ and $b(k) = d(k)$ for $k \neq iM$ $\{k = \pm 1, \pm 2, \dots\}$ where $d(k)$ is the convolutional encoder output assuming values ± 1 .

The received signal is detected with a matched filter whose impulse response is $p^*(-t)/\sqrt{N_0}$, where normalisation by the additive noise power spectral density N_0 is made for notational convenience [1]. The filter output is then given by

$$\begin{aligned} r(k) &= \frac{Ac(kT)}{\sqrt{N_0}} b(k) + n(kT) \\ &= u(k)b(k) + n(k) \end{aligned} \quad (2)$$

where $n(k)$ is the additive white Gaussian noise with unit variance and $c(kT)$ is the piecewise-constant approximation to a multiplicative, zero mean, complex, stationary Gaussian random process $c(t)$. The autocorrelation function of $c(t)$ is given by, assuming a land mobile channel model,

$$R_c(\tau) = \sigma_c^2 J_0(2\pi f_d \tau) \quad (3)$$

where σ_c^2 is the variance of $c(t)$ and f_d is the maximum Doppler spread [1]. The received SNR can be defined by, assuming rate R_0 convolutional coded BPSK,

$$\gamma_b = \frac{E_b}{N_0} = \frac{1}{R_0} \frac{\sigma_c^2 A^2}{N_0} \frac{M}{M-1} \quad (4)$$

which follows from the fact that one frame consists of $M-1$ coded bits and one pilot bit. The variance of $u(k)$ is then given by

$$\sigma_u^2 = R_0 \gamma_b \frac{M-1}{M} \quad (5)$$

Because $c(t)$ is a wide sense stationary Gaussian process, in Reference 1 a Wiener filter was proposed to interpolate $u(k)$ for $k \neq iM$ given the noise corrupted pilot symbol sequence $u(iM) + n(iM)$. Without loss of generality, we can write the interpolation equations for the first frame as subsequent frames would be analysed identically. Therefore, considering the first frame, for $k = 1, \dots, M-1$ the Wiener filter estimates $u(k)$ in eqn. 2 using K pilot samples [1]:

$$\begin{aligned} v(k) &= \sum_{i=-\lfloor K/2 \rfloor}^{\lfloor K/2 \rfloor} h^*(i, k) r(iM) \\ &= \mathbf{h}^\dagger(k) \mathbf{r} \end{aligned} \quad (6)$$

where the dagger denotes conjugate transpose and \mathbf{r} is the length K column vector consisting of the set of pilot samples $r(iM)$, $-\lfloor K/2 \rfloor \leq i \leq \lfloor K/2 \rfloor$. The position-dependent filter coefficients $h(k)$ are determined according to the normal equation [1]

$$\mathbf{R} \mathbf{h}(k) = \mathbf{w}(k) \quad \text{for } k = 1, \dots, M-1 \quad (7)$$

where

$$\mathbf{R} = \frac{1}{2} E[\mathbf{r} \mathbf{r}^\dagger] \quad \text{and} \quad \mathbf{w}(k) = \frac{1}{2} E[u^*(k) \mathbf{r}] \quad (8)$$

Now in this coded scheme, the error rate is dependent on how well $r(k)$ and $v(k)$ are correlated, and the normalised corre-

lation coefficient is [1]

$$\rho(k) = \frac{\mathbf{w}^\dagger(k) \mathbf{R}^{-1} \mathbf{w}(k)}{\sqrt{[(\sigma_u^2 + 1) \mathbf{w}^\dagger(k) \mathbf{R}^{-1} \mathbf{w}(k)]}} \quad (9)$$

Now both $\rho(k)$ and $\sigma_u^2(k)$, the variance of $v(k)$, are clearly position dependent. However, the variation of these across a frame is very low, for example $\sim 0.02\%$ for the PSAM scheme considered later in this Letter. Hence, we ignore this variation and assume $\rho = \rho(1)$ and $\sigma_u = \sigma_u^2(k)$ to be the nominal values for all k . This assumption considerably simplifies the analysis as it makes the decision variable of the Viterbi decoder consist of identically distributed terms.

With the channel estimates $v(k)$, the Viterbi decoder will use the metric $|\mathbf{r}_k - v(k) \mathbf{d}_k|^2$, which would be maximum likelihood if $v(k)$ were a perfect estimate of $u(k)$, and the decision rule for two codewords C_i and C_j having components d_k and \hat{d}_k ($k = 1, \dots, L$) is to choose C_i if $\sum |\mathbf{r}_k - v(k) \mathbf{d}_k|^2 \leq \sum |\mathbf{r}_k - v(k) \hat{\mathbf{d}}_k|^2$. Clearly, only the components of the two codewords that differ contribute to this decision rule. On simplification of this decision rule, it can be readily shown that the decision variable would be

$$U = \text{Re} \left[\sum_{\mathbf{w}} \mathbf{r}(k) v(k)^* (\mathbf{d}_k - \hat{\mathbf{d}}_k) \right] \quad (10)$$

where w is the Hamming distance between C_i and C_j . In the above, $\mathbf{r}(k)$ and $v(k)$ are a pair of correlated complex Gaussian random variables, with all w pairs mutually statistically independent and identically distributed (due to the assumptions of full interleaving and no variation of $\sigma_u(k)$ and $\rho(k)$). Because U is a special case of the general quadratic form given in Reference 4, we can use the results derived there. The pairwise error probability is [4]

$$\begin{aligned} P_d(C_i, C_j) &= \Pr(U < 0) \\ &= \left(\frac{1-\rho}{2} \right)^{2w-1} \sum_{k=0}^{w-1} \binom{2w-1}{k} \left(\frac{1+\rho}{1-\rho} \right)^k \end{aligned} \quad (11)$$

Whereas the above provides the exact pairwise error probability, it is convenient to find an upper bound of the pairwise error probability. Using the Chernoff bound $\{\Pr[U < 0] \leq E(e^{\lambda U})\}$ it can be readily shown that

$$P_d(C_i, C_j) \leq (1 - \rho^2)^w \quad (12)$$

Having determined the pairwise error probability, the next step is to use the union bound on the bit error probability. The average bit error probability $E(P_b)$ of a rate $R_0 = b/v$ linear convolutional code can be bounded as [4]

$$E[P_b] < \frac{1}{b} \frac{dT(D, N)}{dN} \Big|_{N=1, D=\delta} \quad (13)$$

where $T(D, N)$ denotes the standard transfer function of the code, and δ varies according to the detection method. For comparison, it is given by

$$\delta = \begin{cases} (1 - \rho^2) & \text{PSAM} \\ 1/(1 + \gamma_b) & \text{ideal coherent detection} \\ [(1 - \mu^2) \gamma_b^2] \\ + (1 + 2\gamma_b)/(1 + \gamma_b)^2 & \text{differential detection [5]} \end{cases} \quad (14)$$

where μ is the normalised coefficient between adjacent fading variables, given by $\mu = J_0(2\pi f_d T_s)$ for land mobile channels. As an aside, for ideal coherent and differential detection, the upper bound in eqn. 13 can be tightened by a factor of 2. Finally, with the use of eqns. 9, 12 and 13, the error rate performance of any linear convolutional coded binary PSAM can be analysed.

Example: As an example, for binary PSAM coded with a rate $R_0 = \frac{1}{2}$, $K = 3$ optimum convolution code, the bit error probability is computed. For this code, the transfer function $T(D, N)$ is given in Reference 6. We consider a PSAM scheme with

the frame size $M = 7$, the number of pilot samples $K = 11$, and normalised Doppler fading bandwidths 5, 1 and 0.1%. Using eqns. 9, 13 and 14, Fig. 2 has been plotted, with the coefficients optimised at each Doppler bandwidth. We see that, even at 5% Doppler fading bandwidth, coded PSAM requires only 3.5 dB more than coherent detected coded system whereas at 1% Doppler fading the loss is ~ 2 dB. The same amount of loss has been obtained in Reference 1 for uncoded systems. Also, it is seen that coded PSAM has no error floor whereas coded DPSK has. Although the number of pilot samples K has been fixed at 11 for this example it can be as low as 5, as noted in References 1 and 3, if the anticipated worst case Doppler is small ($< 1\%$). This is the typical case in practice. By reducing the number of pilot samples, the required interleaving depth can also be reduced.

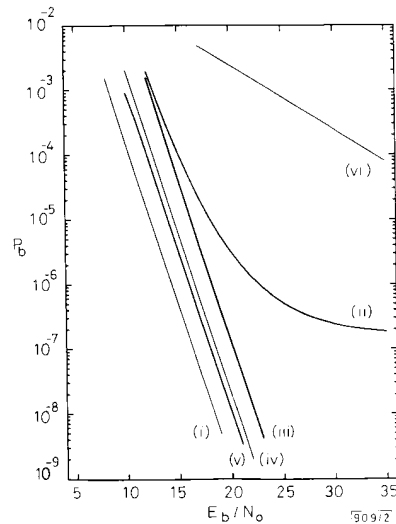


Fig. 2 Bit error probability for $R = 1/2$ and $K = 3$ convolutional code with different modulation techniques in Rayleigh fading

- (i) coherent
- (ii) differential (5% fading bandwidth assumed)
- (iii) PSAM 5%
- (iv) PSAM 1% (very slow fading and perfect coherent detection assumed)
- (v) PSAM 0.1%
- (vi) uncoded

Conclusions: This Letter derives bit error performance for convolutionally coded binary PSAM over Rayleigh fading channels. It compares well with unattainable coherently detected coded BPSK requiring only 3.5 dB more at 5% Doppler fading bandwidth. Also, PSAM outperforms coded differential detection and removes error floors completely. Finally, it provides a significant coding gain over uncoded coherent BPSK.

5th May 1992

C. Tellambura and V. K. Bhargava (Department of Electrical & Computer Engineering, University of Victoria, PO Box 3055, Victoria, BC V8W 3P6, Canada)

References

- 1 CAVERS, J. K.: 'An analysis of pilot symbol assisted modulation for Rayleigh fading channels', *IEEE Trans.*, 1991, VT-40, pp. 686-693
- 2 MOHER, M. L., and LODGE, J. H.: 'TCMP—a modulation and coding strategy for Rician fading channels', *IEEE J. Sel. Areas Commun.*, 1989, SAC-7, pp. 1347-1355
- 3 SAMPEL, S., and SUNAGA, T.: 'Rayleigh fading compensation method for 16QAM in digital land mobile radio channels'. Proc. IEEE Veh. Technol. Conf., San Francisco, CA, May 1989, pp. 640-646
- 4 PROAKIS, J. G.: 'Digital communications' (McGraw-Hill, 1983), pp. 228, 301
- 5 KAM, P. Y.: 'Bit error probabilities of MDPSK over the non-selective Rayleigh fading channel with diversity reception', *IEEE Trans.*, 1991, COM-39, pp. 220-224

ELECTRONICS LETTERS 30th July 1992 Vol. 28 No. 16

6 ODENWALDER, J. P.: 'Optimum decoding of convolutional codes'. PhD Dissertation, Syst. Sci. Dept., Univ. California, Los Angeles, 1970, p. 55

OPTICAL LOOP MIRROR WITH SEMICONDUCTOR LASER AMPLIFIER

M. Eiselt

Indexing terms: Optical amplifiers, Semiconductor lasers, Lasers

A nonlinear optical loop mirror is reported, employing a semiconductor laser amplifier (SLA). The input-output characteristic is distinctly nonlinear, and when operating as an optical correlator, an extinction ratio of 13 dB was achieved.

Introduction: Nonlinear elements serve as important building blocks in various optical signal processing applications. Such applications include the decoding of CDMA encoded signals [1] and the decoding of time interval encoded headers in ATM switching systems [2-4].

In this Letter a new nonlinear element for all-optical signal processing is introduced. The nonlinear element consists of a semiconductor laser amplifier in a loop mirror configuration (SLALOM). The optical nonlinearity is provided by gain saturation of the semiconductor laser amplifier (SLA). A similar setup was demonstrated by O'Neill *et al.* using an asymmetric arrangement of the SLA [5], but unlike this, the SLALOM makes use of the temporal coincidence of two pulses and thus allows a correlation operation. Compared to fibre Sagnac loop mirrors (see, for example Reference 6), where a long (several kilometres) optical fibre acts as the optical nonlinear element, the SLALOM could be integrated on a chip. The operation of the SLALOM for contrast enhancement and as an optical correlator for picosecond pulses is demonstrated in this work.

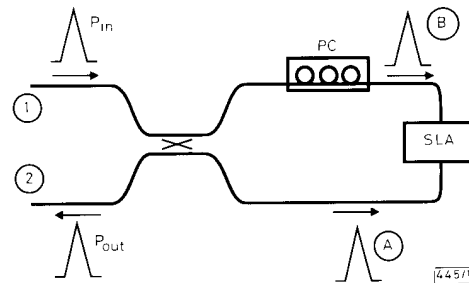


Fig. 1 Principle of operation of SLA loop mirror

Principle of operation of SLALOM: Fig. 1 depicts the basic elements of the SLALOM. It consists of a 3 dB coupler with two arms connected forming a loop. The loop contains a polarisation controller (PC) and a semiconductor laser amplifier (SLA). If the SLA were not in the loop and with an ideal 50:50 coupler, an optical pulse injected to port 1 would be split equally to both branches of the loop. With a properly adjusted polarisation controller and after travelling equal paths through the loop, both pulses would cancel each other at port 2 due to their opposite phase relations. With a non-equally splitting coupler, the cancellation is incomplete at port 2, and the power of output pulse P_{out} is proportional to the input power P_{in} .

Now consider a loop with an SLA, whose position is selected so that the propagation time from the coupler to the SLA via one branch of the loop is shorter than the propagation time via the other arm by a small time difference Δt . Again a single input pulse is split by the coupler into two pulses. One of the two pulses in the loop, pulse B in Fig. 1 for example, will arrive earlier at the SLA than pulse A. Pulse B is ampli-

1505